Semiclassical analysis of the Bogoliubov spectrum in the Bose-Hubbard model

Andrey R. Kolovsky

Kirensky Institute of Physics, 660036 Krasnoyarsk, Russia
(Received 3 May 2007; published 13 August 2007)

We analyze the Bogoliubov spectrum of the Bose-Hubbard model with a finite number of sites and Bose particles by using a semiclassical approach. This approach allows us to take into account the finite-size effects responsible for evolution of the Bogoliubov spectrum into an irregular (chaotic) spectrum at higher energies. A manifestation of this transition for the excitation dynamics of the Bose-Hubbard system is discussed as well.

I. INTRODUCTION

The Bose-Hubbard model (BH model) constitutes one of the fundamental Hamiltonians in the condensed matter theory. The number of phenomena, discussed in the frame of the BH model, is so diverse that sometimes it is difficult to see any link between them. In particular, this concerns phenomena of superfluidity and quantum chaos. Indeed, the former phenomenon assumes a phononlike excitation spectrum, described by Bogoliubov theory [1,2], while the latter phenomenon implies a highly irregular excitation spectrum, described by the random matrix theory [3–6]. This seeming contradiction is resolved by noting that these two spectra refer to different characteristic energies of the system. It is the aim of the present work to understand (i) how the regular Bogoliubov spectrum evolves into an irregular one as the system energy is increased and (ii) how this transition might be related to superfluidity of the BH system.

To approach the outlined problems we first consider the simplest nontrivial case of the 3-sites BH model. Indeed, as shown below in Sec. II, the 3-sites BH model can be formally treated by using Bogoliubov theory but, at the same time, is known to be chaotic. The fact that the 3-sites BH model is a chaotic system follows from the simple classical arguments, where it is viewed as a system of three coupled nonlinear oscillators [7–11]. Since one has only two conserved quantities (the energy E and the number of particles N) for three degrees of freedom, the system cannot be integrated [12]. We revisit the problem of chaos in the 3-sites BH model in Sec. IV, where we show that, along with the chaotic component, the system has two regular components, associated with low and high energies. Here the additional local integrals of motion exist, and for the low-energy regular component we find these integrals explicitly. Moreover, quantizing them, we obtain the Bogoliubov spectrum as well as the finite-N corrections to this spectrum (Secs. III–V).

Thanks to a relatively low dimensionality of the 3-sites BH model, it can be exhaustively analyzed, both classically and quantum mechanically. Unfortunately, this is not the case for the L-sites BH system. To get a feeling of how generic the results are on the 3-sites system, we consider in Sec. VI the next complexity case of the 5-sites BH model. A qualitative difference between the 3-sites and 5-sites BH models is that the latter system has two different Bogoliubov frequencies and, hence, two Bogoliubov spectra. We analyze interactions between Bogoliubov spectra, which may consid-

erably affect the onset of quantum chaos. In particular, the critical energy separating the regular and chaotic spectra is lowered by one order of magnitude as compared to the 3-sites system.

Finally, in Sec. VII we touch upon the problem of superfluidity in the finite-L BH system. In the elementary level this problem can be reformulated as the system response to an external perturbation such as, for example, dragging an impurity through the superfluid [13]. We consider a particular external perturbation in the form of harmonic driving of the BH system. (To some extent, this mimics excitations by dragging an impurity, where the dragging velocity is associated with the frequency of harmonic driving.) Clearly, if the driving frequency is close to the Bogoliubov frequency, the system may be excited from its ground state. Depending on the system parameters, we have observed two qualitatively different regimes of excitations, reversible and irreversible, which are explained in terms of the regular and chaotic energy spectrum.

II. THE BOGOLIUBOV SPECTRUM

The Bogoliubov spectrum describes elementary excitations of the interacting Bose particles. The standard derivation of this spectrum involves an expansion of the field operator near the mean-field solution, followed by the Bogoliubov–de Gennes transformation. The method is simple but has two drawbacks. First, it ignores the conservation law for the particle number and, second, being rather formal it hides the underlying classical dynamics of the system. In this section, following Ref. [6], we introduce the Bogoliubov spectrum in a different way, which is free from the above-mentioned drawbacks and is particularly suited for our present aims.

To be concrete, we shall discuss the Bogoliubov spectrum with respect to the 3-sites BH model,

$$\hat{H} = -\frac{T}{2}\sum_{l=1}^{L=3}(\hat{a}_{l+1}^{\dagger}\hat{a}_l + \text{H.c.}) + \frac{U}{2}\sum_{l=1}^{L=3}\hat{a}_l^{\dagger}\hat{a}_l^{\dagger}\hat{a}_l\hat{a}_l, \quad (1)$$

although the approach is valid for arbitrary L. Using the canonical transformation $\hat{b}_k = (1/\sqrt{L})\Sigma_l \exp(i2\pi kl/L)\hat{a}_l$, the Hamiltonian (1) takes the form

$$\hat{H} = -T\sum_k \cos\left(\frac{2\pi k}{L}\right)\hat{b}_k^\dagger \hat{b}_k$$

$$+ \frac{U}{2L}\sum_{k_1,k_2,k_3,k_4} \hat{b}_{k_1}^\dagger \hat{b}_{k_2}^\dagger \hat{b}_{k_3} \hat{b}_{k_4} \tilde{\delta}(k_1 + k_2 - k_3 - k_4), \quad (2)$$

where $\tilde{\delta}(k)=1$ if k is a multiple of L and $\tilde{\delta}(k)=0$ otherwise. For $L=3$ the Hilbert space of (2) is spanned by the quasimomentum Fock states $|n_{-1}, n_0, n_{+1}\rangle$, where $\Sigma_k n_k = N$, the total number of particles.

For $U=0$ the ground state of (2) is the product state $|\Psi_0\rangle = |0, N, 0\rangle$, where all particles have zero quasimomentum. The energy of this state is $E_{GP} = -TN + UN(N-1)/2$, which is often referred to as the mean-field or Gross-Pitaevskii ground energy. (From now on we shall measure the system energy with respect to this energy.) For $U \neq 0$, to find the ground and first excited states of the system, one uses the ansatz [2]

$$|\Psi\rangle = \sum_{n=0}^{N/2} c_n |n, N-2n, n\rangle. \quad (3)$$

Substituting (3) in (2) and assuming the limit $N \to \infty$, $U \to 0$, $g = UN/L = $ const, we obtain the following equation on the coefficients c_n:

$$2(\delta + g)nc_n + gnc_{n-1} + g(n+1)c_{n+1} = Ec_n, \quad (4)$$

where $g = NU/L$ and $\delta = T[\cos(2\pi/3) - 1] = 1.5T$ are the so-called macroscopic interaction constant and single-particle excitation energy, respectively. The matrix equation (4) can be solved analytically by mapping it to a differential equation. Namely, introducing the generating function $\Phi(\theta) = (1/\sqrt{2\pi})\Sigma_n c_n e^{in\theta}$, we have

$$\hat{H}_{eff}\Phi(\theta) = E\Phi(\theta), \quad \Phi(\theta + 2\pi) = \Phi(\theta), \quad (5)$$

$$\hat{H}_{eff} = 2(\delta + g)\hat{n} + g(e^{-i\theta}\hat{n} + \hat{n}e^{i\theta}), \quad \hat{n} = -i\,\partial/\partial\theta. \quad (6)$$

The spectrum of the eigenvalue problem (5) is given by $E_n = E_0 + 2\Omega n$ [6], where $\Omega = \sqrt{2g\delta + \delta^2}$ is the celebrated Bogoliubov frequency and $E_0 = -\Omega/2 + (\delta + g)$ is the Bogoliubov correction to the Gross-Pitaevskii ground energy ($E_0 < 0$).

It should be mentioned that, instead of (3), one can use a slightly different ansatz,

$$|\Psi\rangle = \sum_n c_n |n, N-2n-p, n+p\rangle, \quad (7)$$

which modifies Eq. (4) as

$$(\delta + g)(2n+p)c_n + g\sqrt{n(n+p)}c_{n-1}$$
$$+ g\sqrt{(n+1)(n+p+1)}c_{n+1} = Ec_n. \quad (8)$$

The spectrum of (8) is again linear but is shifted with respect to the previous spectrum by p quanta of the Bogoliubov frequency,

$$E_{n,p} = E_0 + \Omega(2n + p). \quad (9)$$

As a consequence of the last equation, excited energy levels of the Bogoliubov spectrum are multiple degenerate. To deal
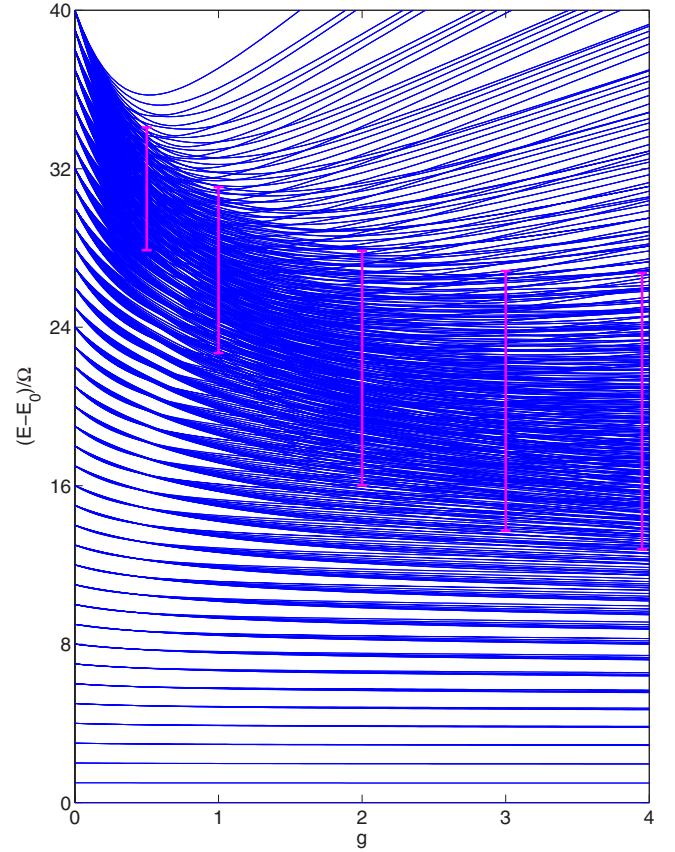
FIG. 1. (Color online) Energy spectrum of the 3-sites BH model for $N=40$. The energy is measured with respect to the ground energy E_0 and scaled with respect to the Bogoliubov frequency Ω. Error bars indicate energy intervals, where the classical counterpart of the system shows chaotic dynamics.

with this degeneracy it is convenient to introduce instead of the quantum numbers n and p a different set of the quantum numbers: the number m, which counts Bogoliubov levels begging from the ground state $m=0$, and the number j, which labels the degenerate sublevels of the mth level. To fix notations we shall call the number m by primary quantum number and the number j by secondary quantum number. This second quantum number takes integer values for even m and half-integer values for odd m in the interval $|j| \leq m/2$. Thus we have

$$E_{m,j} = E_0 + \Omega m, \quad \Omega = \sqrt{2g\delta + \delta^2}, \quad |j| \leq m/2. \quad (10)$$

The corresponding to (10) wave functions are denoted by $|\Psi_{m,j}\rangle$, where $|\Psi_{m,j}\rangle = |m/2 - j, N-m, m/2 + j\rangle$ for $g=0$. Thus the second quantum number j is associated with the mismatch in population of $k=-1$ and $k=+1$ quasimomentum states.

Concluding this section, we would like to stress that the above result is valid only in the limit of infinite N and for any finite N the low-energy spectrum of the BH-model deviates from the Bogoliubov spectrum (10). As an illustration to this statement, Fig. 1 shows the energy spectrum of the 3-sites BH model for $N=40$ and $0 \leq g \leq 4$. It is seen in the figure that (i) the spectrum is not linear, and (ii) Bogoliubov levels

are split with respect to the secondary quantum number. In the subsequent sections we shall quantify both of these effects by using a semiclassical approach. This approach will also allow us to indicate the critical energy, above which the spectrum of the BH model is chaotic.

III. SEMICLASSICAL APPROACH

As an intermediate step we shall derive the Bogoliubov spectrum by using the semiclassical arguments. The classical counterpart of the Hamiltonian (2) is obtained by scaling it with respect to the total number of particles, $\hat{H}/N \rightarrow H$, and identifying the operators $\hat{b}_k^\dagger / \sqrt{N}$ and $\hat{b}_k / \sqrt{N}$ with pairs of canonically conjugated variables (b_k^*, b_k). Thus, we have

$$H = -T \sum_{k=-1}^{1} \cos\left(\frac{2\pi k}{3}\right) b_k^* b_k$$

$$+ \frac{g}{2} \sum_{k_1, k_2, k_3, k_4} b_{k_1}^* b_{k_2}^* b_{k_3} b_{k_4} \widetilde{\delta}(k_1 + k_2 - k_3 - k_4). \quad (11)$$

Next we change to the action-angle variables, $b_k = \sqrt{I_k} \exp(i\theta_k)$, which provide a better insight into the system dynamics. In these variables the Hamiltonian (11) reads

$$H = \sum_k \left(-T \cos(2\pi k/3) I_k + \frac{g}{2} I_k^2 \right) + 2g \sum_{k \neq k'} I_k I_{k'}$$

$$+ 2g \sum_{k \neq k' \neq k''} I_k \sqrt{I_{k'} I_{k''}} \cos(2\theta_k - \theta_{k'} - \theta_{k''}). \quad (12)$$

Taking into account that $I_0 + I_{+1} + I_{-1} = 1$ is an integral of the motion, this system of three degrees of freedom can be reduced to the system of only two degrees of freedom. Indeed, measuring the phases $\theta_{\pm 1}$ with respect to the phase θ_0, we have

$$\dot{\theta}'_{\pm 1} = \dot{\theta}_{\pm 1} - \dot{\theta}_0 = \frac{\partial H}{\partial I_{\pm 1}} - \frac{\partial H}{\partial I_0} = \frac{\partial H'}{\partial I_{\pm 1}},$$

where $H' = H'(I_{\pm 1}, \theta_{\pm 1})$ is obtained from the Hamiltonian (12) by substituting there $I_0 = 1 - I_{+1} - I_{-1}$ and setting θ_0 to zero. In what follows we drop the prime sign, i.e., H always refers to the Hamiltonian of the reduced system of two degrees of freedom.

As mentioned in Sec. II, the Bogoliubov spectrum describes the low-energy excitations, where $n_{\pm 1}$ is much smaller than n_0, the number of particles in the $k=0$ quasimomentum state. Semiclassically, the latter condition means $I_{\pm 1} \ll I_0 \sim 1$. Keeping in the Hamiltonian $H = H(I_{\pm 1}, \theta_{\pm 1})$ only the first-order terms on $I_{\pm 1}$, we have (up to an additive constant)

$$H \approx (\delta + g)(I_{+1} + I_{-1}) + 2g\sqrt{I_{+1} I_{-1}} \cos(\theta_{+1} + \theta_{-1}), \quad (13)$$

where, as before, $\delta = T[1 - \cos(2\pi/3)] = 3T/2$. Next, using the canonical transformation,

$$I = I_{+1}, \quad \theta = \theta_{+1} + \theta_{-1},$$

$$(14)$$

$$P = I_{+1} - I_{-1}, \quad \vartheta = (\theta_{+1} - \theta_{-1})/2,$$

we reduce the Hamiltonian (13) to

$$H_{\text{eff}} = (\delta + g)(2I + P) + 2g\sqrt{I(I + P)} \cos\theta. \quad (15)$$

Since H_{eff} in Eq. (15) does not depend on ϑ, the action P is an integral of the motion. It is also straightforward to see that P corresponds to the number p in the quantum problem (8). In particular, if we set $P=0$, the Hamiltonian (15) coincides with the classical counterpart $(\hat{n}/N \rightarrow I)$ of the effective Hamiltonian (6),

$$H_{\text{eff}} = 2(\delta + g)I + 2gI \cos\theta. \quad (16)$$

Finally, we integrate the system (16) by introducing a new action,

$$\widetilde{I} = \frac{1}{2\pi} \oint I(\theta, \widetilde{E}) d\theta, \quad (17)$$

and resolving Eq. (17) with respect to the energy $\widetilde{E} = E/N$. We have

$$\widetilde{I} = \frac{1}{2\pi} \oint \frac{\widetilde{E}}{2\delta + 2g(1 + \cos\theta)} d\theta = \frac{\widetilde{E}}{2\Omega}, \quad (18)$$

or $\widetilde{E} = 2\Omega\widetilde{I}$. Generalization of this result to nonzero P provides the degenerate Bogoliubov spectrum $\widetilde{E} = \Omega(2\widetilde{I} + P)$.

Concluding this section we mention that, instead of the transformation (14), one can use a different canonical transformation,

$$I = I_{+1} + I_{-1}, \quad \theta = (\theta_{+1} + \theta_{-1})/2,$$

$$J = (I_{+1} - I_{-1})/2, \quad \vartheta = \theta_{+1} - \theta_{-1}, \quad (19)$$

which corresponds to the labelling of Bogoliubov levels by the quantum numbers m and j. Then the low-energy Hamiltonian has the following form:

$$H_{\text{eff}} = (\delta + g)I + g\sqrt{I^2 - 4J^2} \cos(2\theta). \quad (20)$$

Integrating the system (20) we again get linear dependence of the energy on the action $\widetilde{I}$,

$$\widetilde{E} = \Omega\widetilde{I}, \quad \widetilde{I} \ll 1. \quad (21)$$

However, now the energy is independent of the integral of the motion J, which may be chosen arbitrarily in the interval $|J| \le \widetilde{I}/2$.

IV. TRANSITION TO CHAOS

The results of the preceding section refer to the limiting case of low energies, where $I_k \ll 1$ ($k \neq 0$). With an increase of energy, as it was already mentioned in the introduction, the BH system shows a transition to chaos. In this section we revisit the problem of chaos in the 3-sites BH model [3,5]. Through the section we shall use the canonical substitution (19). After this substitution (and taking into account that $I_0 = 1 - I$) the classical Hamiltonian (12) takes the following form:
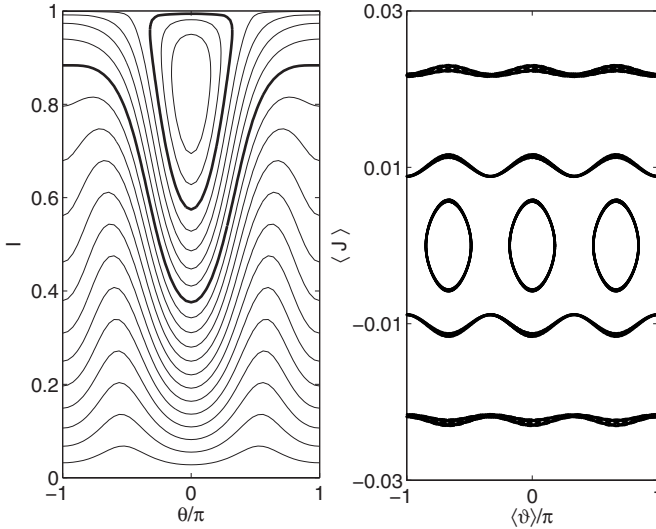
FIG. 2. Left-hand side: phase portrait of the 1D system (23) for $g=1$. Bold lines restrict the chaotic region, where trajectories are unstable with respect to the variation of (J, ϑ). Right-hand side: slow dynamics of the variables $\bar{J}=\langle J \rangle$ and $\bar{\vartheta}=\langle \vartheta \rangle$ for $g=1$ and $\widetilde{I}=0.133$.

$$H = \delta I + g \left[\frac{1}{2} + I - \frac{3}{4}I^2 - J^2 + 2(1-I)\sqrt{\frac{I^2}{4} - J^2}\cos(2\theta) \right.$$
$$+ 2\sqrt{1-I}\left(\frac{I}{2}+J\right)\sqrt{\frac{I}{2}-J}\cos\left(\theta + \frac{3}{2}\vartheta\right)$$
$$\left. + 2\sqrt{1-I}\left(\frac{I}{2}-J\right)\sqrt{\frac{I}{2}+J}\cos\left(\theta - \frac{3}{2}\vartheta\right) \right]. \quad (22)$$

First we shall analyze the symmetric solutions $b_{+1}(t) = b_{-1}(t)$. The imposed condition means that one should set $J=0$ and $\vartheta=0$ in the Hamiltonian (22). The resulting effective one-dimensional (1D) Hamiltonian reads as follows:

$$H_{1D} = (\delta+g)I + g(1-I)I\cos(2\theta) - 3gI^2/4$$
$$+ gI\sqrt{2(1-I)I}\cos(\theta). \quad (23)$$

For $g=1$ the phase portrait of the 1D system (23) is depicted in Fig. 2(a). Our particular interest in this phase portrait are trajectories near the origin $I=0$, which can be associated with the Bogoliubov states. It is seen in the figure that these trajectories are strongly affected by the elliptic point in the upper part of the phase space. (It is worth mentioning that with further increase of g, the second elliptic point appears at $\theta = \pm\pi$ and $I \approx 0.5$.) As a consequence, the eigenfrequency of the system depends on the action $\widetilde{I}$. Namely, $\widetilde{\Omega}=\widetilde{\Omega}(\widetilde{I})$ vanishes for the separatrix action $\widetilde{I}^*$, and for $\widetilde{I} \ll \widetilde{I}^*$ one has

$$\widetilde{\Omega}(\widetilde{I}) = \Omega - \gamma\widetilde{I}, \quad (24)$$

where the nonlinearity γ is a unique function of g. (For example, $\gamma/\Omega = 0.1, 0.6, 1$ for $g=0.1, 1, 4$.) Referring to the quantum problem, the result (24) means that the energy difference between $(m+1)$th and mth Bogoliubov levels decreases as $\gamma m/N$.
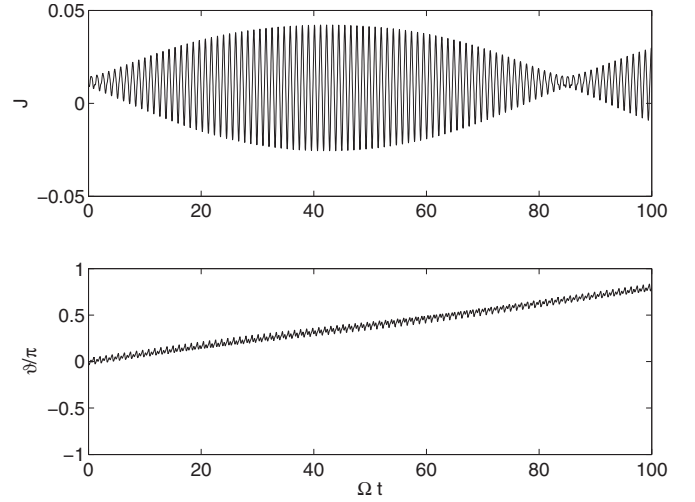
FIG. 3. Time evolution of the conjugated variables J and ϑ for $g=1$. The initial conditions are $(I(0), \theta(0))=(0.08,0)$, $(J(0), \vartheta(0)) = (0.01,0)$.

Next we address the stability of phase trajectories depicted in Fig. 2 with respect to variation of J. Within the approach of Sec. III (where we discussed the limiting case $I \ll 1$), the action J is an integral of the motion and may be chosen arbitrarily in the interval $|J| \le \widetilde{I}/2$. It should be understood, however, that this is an approximation and in reality the action J does depend on time. An example of this dependence is given in Fig. 3. It is seen that time evolution is a superposition of fast dynamics, where $J(t)$ and $\vartheta(t)$ oscillate with the Bogoliubov frequency (more precisely, with the frequency $\widetilde{\Omega}$), and slow dynamics, with the characteristic frequency of the orders of magnitude smaller than the Bogoliubov frequency. Going ahead, we note that this new frequency defines the splitting of Bogoliubov levels in Fig. 1, and for the moment we only stress that the system dynamics remains regular. To support this statement, Fig. 4(a) shows the Poincaré cross section of the system (22) by the plane $\theta=0$. We come back to this regular regime in the next section.

The stability phase portrait depicted in Fig. 4(a) is typical for any trajectory of the effective 1D system (23), providing the trajectory lies well below the separatrix. If we choose a trajectory closer to the separatrix, we observe a transition from regular to chaotic dynamics [see Fig. 4(b)]. We identify the border of chaos by using the standard Monte Carlo approach. Namely, generating initial conditions $(I_{\pm1}, \theta_{\pm1})$ at random and running this trajectory for a long time, we build up the Poincaré cross section of the system (11) by the plane θ_{-1}. [Numerically it is more convenient to work with the original variables $b_k = \sqrt{I_k}\exp(i\theta_k)$, without doing the canonical transformation (19).] The maximally available cross section volume, given by $0 < I_{+1} < 1$ and $-\pi < \theta_{+1} < \pi$, is divided by $Q \times Q$ equal cells and we count the number of cells $q(t)$ visited by the trajectory. Clearly, the number of visited cells is of the order of Q, if the trajectory is regular, and essentially exceeds this characteristic value if the trajectory is chaotic. The results of the described Monte Carlo simula-
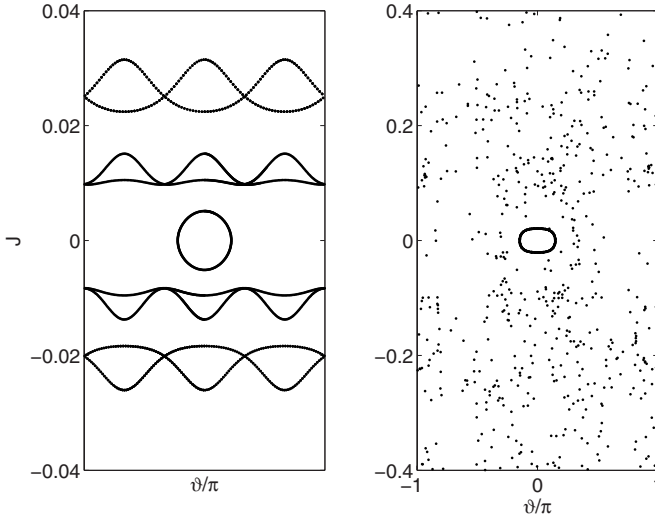
FIG. 4. Stability phase portrait for $g=1$ and $(I(0),\theta(0))$ $=(0.08,0)$ (left-hand side) and $(I(0),\theta(0))=(0.4,0)$ (right-hand side). Cross section by the plane $\theta=0$ of five different trajectories is shown. (The crossing of trajectories is an artificial fact caused by folding them into the interval $-\pi \leq \vartheta < \pi$.)

tions are depicted in the lower panel of Fig. 5 for $g=1$. It is seen in the figure that the chaotic region is restricted to a relatively narrow energy interval $0.75 < \widetilde{E} < 1.25$. In Fig. 2(a) we mark by bold lines the phase trajectories of the effective 1D system, corresponding to boundaries of this energy interval. Thus a finite perturbation of a symmetry-plane trajectory, located between the bold lines, typically makes the dynamics chaotic. On the contrary, outside the marked region, the symmetry plane trajectory is stable with respect to a finite perturbation.

Using the above method, we determined chaotic regions for different values of the interaction constant g. The result of these extensive numerical studies is summarized by the
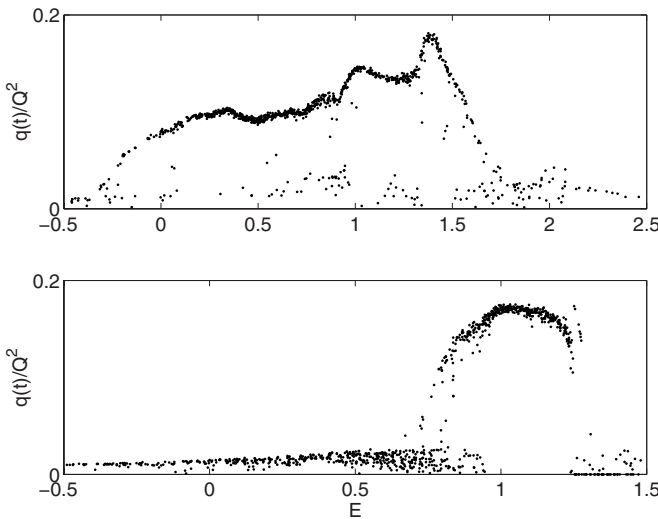
FIG. 5. Fraction of the cross-section phase volume, visited by the trajectory with given energy $\widetilde{E}$ after $t \approx 5000$ crossings for L $=3$ (bottom) and $L=5$ (top).
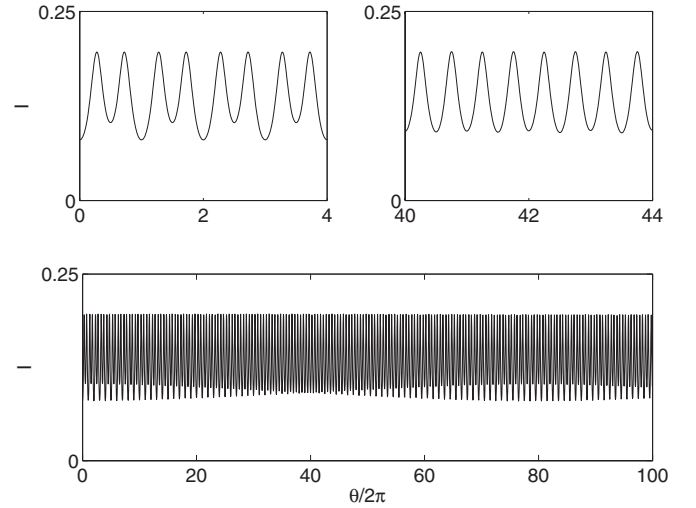
FIG. 6. Dependence of the action I on the conjugated phase θ for the parameters of Fig. 3. The upper subplots zoom in the depicted dependence around $\theta=0$ and $\theta/2\pi=40$.

error bars in Fig. 1. The depicted borders are consistent with visual analysis of the spectrum and suggest the following simple criteria of the transition to chaos: it takes place when the splitting of Bogoliubov levels with respect to the second quantum number j exceeds the mean distance $\widetilde{\Omega}$ between the levels.

V. SPLITTING OF THE BOGOLIUBOV LEVELS

To quantify the level splitting, we shall discuss the low-energy regular dynamics of (22) in more detail. First, we note that the action $\widetilde{I}=(1/2\pi)\oint I d\theta$, introduced in Sec. III, is an adiabatic integral of the motion and, hence, does not depend on the second pair of the conjugated variables (J,ϑ). This statement is illustrated in Fig. 6, where we plot I as a function of θ for the parameters of Fig. 3. It is seen in the figure that the square under the curve $I=I(\theta)$ keeps constant for any 2π interval, although the functional dependence itself slowly changes with time. The conjugated to $\widetilde{I}$ variables $\widetilde{\theta}$ defines the fast dynamics of the system through the relation $\widetilde{\theta}=\widetilde{\Omega}t$, where $\widetilde{\Omega}=\widetilde{\Omega}(\widetilde{I})$ is the corrected Bogoliubov frequency.

To address the slow dynamics we introduce new variables $\overline{J}=(1/2\pi)\oint J d\widetilde{\theta}$ and $\overline{\vartheta}=(1/2\pi)\oint \vartheta d\widetilde{\theta}$. (Essentially this amounts to averaging of J and ϑ over one period of the fast dynamics.) Assuming, as before, $I_{\pm} \ll 1$, we obtain from (22),

$$\dot{\overline{\vartheta}} \approx -2g\overline{J},$$

$$\dot{\overline{J}} \approx 3gV(g,\widetilde{I})\sin(3\overline{\vartheta}/2),$$

where

$$V(g,\widetilde{I}) = \langle (I_{+1}\sqrt{I_{-1}} + I_{-1}\sqrt{I_{+1}})\cos\theta \rangle, \quad (26)$$

and $\langle \cdots \rangle$ means time average. Thus, the slow dynamics is defined by a pendulumlike Hamiltonian,

$$H_{\text{slow}} = -g\bar{J}^2 + gV(g,\tilde{I})\cos(3\bar{\vartheta}/2). \tag{27}$$

It is worth noting that, to obtain (27), we have assumed the quantity (26) to be independent of $\bar{J}$, which is justified for $|\bar{J}| \ll \tilde{I}/2$. Nevertheless, the Hamiltonian (27) is found to capture well the main features of the low-energy regular dynamics for arbitrary $\bar{J}$. In particular, it correctly predicts the existence of stable stationary points at $\vartheta = 0, \pm 4\pi/3$, where the relative phase of the complex amplitudes $b_{\pm 1}(t)$ is locked to $0°$ or $\pm 120°$, respectively [see Fig. 2(b)]. The size of the stability islands around these fixed points is obviously given by the pendulum separatrix, i.e., proportional to $|V(g,\tilde{I})|^{1/2}$.

It is instructive to consider the limiting case $g \to 0$. As it is easy to show, in this limit $V(g,\tilde{I}) \to 0$ and, hence, $H_{\text{slow}} = -g\bar{J}^2$. Let us prove that this result corresponds to the first-order quantum perturbation theory on U for the Hamiltonian (2). Indeed, calculating the first-order correction to the energy of the quasimomentum Fock state $|\Psi_{m,j}\rangle = |m/2 - j, N - m, m/2 + j\rangle$, we have

$$\Delta E = \frac{U}{2L}\langle \Psi_{m,j}| \sum_{k_1,k_2,k_3,k_4} \hat{b}_{k_1}^\dagger \hat{b}_{k_2}^\dagger \hat{b}_{k_3} \hat{b}_{k_4} \tilde{\delta}(k_1 + k_2 - k_3 - k_4)|\Psi_{m,j}\rangle$$

$$\sim -\frac{U}{L}j^2, \tag{28}$$

or $\Delta E/N = -g\bar{J}^2$, where $\bar{J} = j/N$. Thus for small g the splitting between sublevels grows linearly with g. This linear regime changes to a nonlinear one as soon as the second term in the Hamiltonian (27) takes a non-negligible value. This second term also causes a rearrangement of the sublevels, clearly seen in Fig. 1. Needless to say that in this case the second quantum number is defined by the action $\tilde{J} = (1/2\pi)\oint \bar{J}d\bar{\vartheta}$, which amounts to the phase volume encircled by trajectories in Fig. 2(b).

We conclude this section by formulating a quantitative criteria for the onset of quantum chaos. As mentioned earlier, the transition to irregular spectrum occurs when the total splitting of the mth Bogoliubov level compares with the Bogoliubov frequency. Ignoring the nonlinear corrections, one has $g(m+1)^2/4N \sim \Omega$, or

$$m_{cr} \approx \left(\frac{4N\sqrt{\delta^2 + 2\delta g}}{g} \right)^{1/2}. \tag{29}$$

Through the relation $E_{cr} \approx \Omega m_{cr}$ this estimate defines the critical energy above which the regular spectrum transforms into a chaotic one. [For example, for $N=40$ the estimates (29) predicts that m_{cr} drops to $m_{cr}=13$ at $g=4$, which should be compared with $m_{cr}=16$ in Fig. 1.]

VI. INTERACTING BOGOLIUBOV SPECTRA

To which extent are the above results on the 3-sites BH model valid for the general case $L > 3$? To answer this question we shall analyze the 5-sites BH model. The 5-sites BH model has two different Bogoliubov frequencies and, hence, may capture additional effects, not present in the 3-sites sys-

tem. In particular, we shall focus on mutual influence of the different Bogoliubov spectra.

To study this mutual influence, we include into consideration the following processes: annihilation of two particles in the $k=0$ quasimomentum state and creation of them in either the states $k=\pm 1$ or $k=\pm 2$; annihilation of two particles in the $k=+1$ quasimomentum state and the creation of them in the states $k=0$ and $k=+2$ (and the symmetric process for $k=-1$); annihilation of two particles in the $k=+2$ quasimomentum state and the creation of them in the states $k=0$ and $k=-1$ (and the symmetric process for $k=-2$). The semiclassical Hamiltonian for these processes reads as follows:

$$H = (\delta_1 + g)(I_{-1} + I_{+1}) + 2g\sqrt{I_{-1}I_{+1}}\cos(\theta_{-1} + \theta_{+1})$$

$$+ (\delta_2 + g)(I_{-2} + I_{+2}) + 2g\sqrt{I_{-2}I_{+2}}\cos(\theta_{-2} + \theta_{+2})$$

$$+ 2gI_{+1}\sqrt{I_{+2}}\cos(2\theta_{+1} - \theta_{+2}) + 2gI_{-1}\sqrt{I_{-2}}\cos(2\theta_{-1} - \theta_{-2})$$

$$+ 2gI_{+2}\sqrt{I_{-1}}\cos(2\theta_{+2} - \theta_{-1}) + 2gI_{-2}\sqrt{I_{+1}}\cos(2\theta_{-2} - \theta_{+1}), \tag{30}$$

where it was implicitly assumed that $I_0 \approx 1$. The first two terms in the Hamiltonian (30) obviously correspond to two independent Bogoliubov spectra, while the rest describes interactions between the spectra. For simplicity, we shall consider only the symmetry plane solutions, i.e., we set in (30) $I_{-1} = I_{+1} \equiv I_1/2$, $\theta_{-1} = \theta_{+1} \equiv \theta_1$ and $I_{-2} = I_{+2} \equiv I_2/2$, $\theta_{-2} = \theta_{+2} \equiv \theta_2$. Considering the terms responsible for interactions in (30) as a perturbation and introducing the actions $\tilde{I}_{1,2} = \oint I_{1,2}d\theta_{1,2}$, we have

$$H = \Omega_1\tilde{I}_1 + \Omega_2\tilde{I}_2 + g\tilde{I}_1\sqrt{2\tilde{I}_2}\cos(2\tilde{\theta}_1 - \tilde{\theta}_2)$$

$$+ g\tilde{I}_2\sqrt{2\tilde{I}_1}\cos(2\tilde{\theta}_2 - \tilde{\theta}_1). \tag{31}$$

It immediately follows from (31) that the mutual influence of spectra (more precisely, the mutual influence of two degrees of freedom, associated with two spectra) is a resonant process, where the resonance condition reads as

$$2\Omega_1(g) = \Omega_2(g). \tag{32}$$

(For the 5-sites BH model this condition is satisfied at $g = 0.7135$.) Moreover, since we are interested in the limiting case $\tilde{I}_{1,2} \ll 1$, the last term in (31) can be safely neglected. Then the quantity $\mathcal{J} = 2\tilde{I}_2 + \tilde{I}_1$ is an integral of the motion and the system can be integrated analytically. We omit this standard analysis and only mention that the integrated dynamics essentially corresponds to periodic oscillations of the actions $\tilde{I}_1$ and $\tilde{I}_2$ with the characteristic frequency $\Omega_{\text{int}} \sim g\mathcal{J}^{1/2}$ (see Fig. 7).

One finds a quantum manifestation of the above-discussed classical dynamics in the form of avoided crossings between Bogoliubov levels. To study this problem systematically, we diagonalize the Hamiltonian of the 5-sites BH model in the truncated quasimomentum Fock basis $|n_{-2}, n_{-1}, n_0 + N'', n_{+1}, n_{+2}\rangle$, where $\Sigma_l n_l = N'$ and $N' + N'' = N$, the total number of particles. Clearly, by using the truncated basis, one can find only the low-energy spectrum. (We control an accuracy by watching the spectrum convergence as the pa-
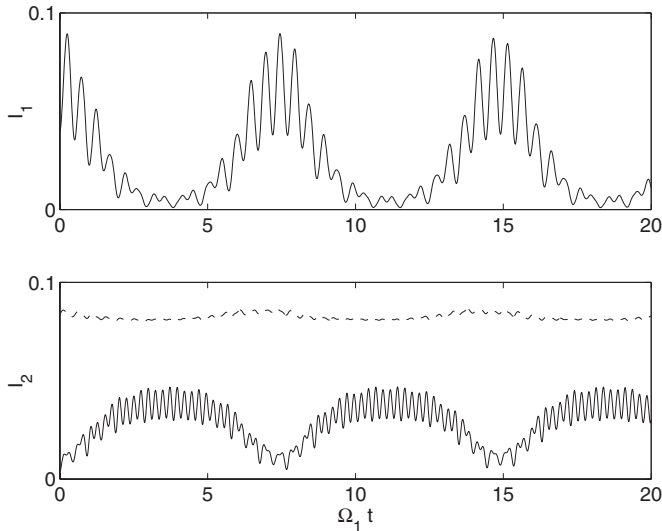
FIG. 7. Classical dynamics of the 5-sites BH model in the near resonant regime ($g=0.5$). The initial conditions are $I_{\pm 1}=0.04$, $\theta_{\pm 1}=0$ and $I_{\pm 2}=0.004$, $\theta_{\pm 2}=0$. The dashed line in the lower subplot shows the quantity $\mathcal{J}=2\tilde{I}_2+\tilde{I}_1\approx\langle 2I_2+I_1\rangle$, which is an integral of the motion in the limit $\tilde{I}_{1,2}\to 0$.

rameter N' is increased.) The upper and lower panels in Fig. 8 show the low-energy spectrum of the 5-sites BH model for $N=101$ and $N=401$, respectively. A number of avoided crossings at $g=0.7135$ is clearly seen. According to the classical estimate for Ω_{int}, the gaps of these avoided crossings scales as $g/\sqrt{N}$ [14], which fully agrees with the depicted numerical results. We also would like to note that interactions between the spectra enhance the splitting of Bogoliubov levels with respect to the second quantum number. Indeed, as shown in Sec. V, this splitting scales as g/N and would not be resolved in the scale of the figure if there were no interactions.

The discussed interactions between two degrees of freedom, associated with two Bogoliubov spectra, also facilitate the transition to chaos at higher energies. The upper panel in Fig. 5 shows results of the symmetry-plane analysis of the 5-sites system. For symmetry-plane trajectories the eight-dimensional phase space of the system is reduced to four dimensions and, thus, we can employ the same method of Poincare cross section as was used earlier in Sec. IV. It is seen in the figure that the border of chaos in the 5-sites BH model is tremendously lowered as compared to the 3-sites system.

VII. EXCITATION DYNAMICS

It has been shown in the preceding sections that for a finite N the regular Bogoliubov spectrum of the finite-L BH model evolves into a chaotic spectrum as the system energy is increased. This has important consequences when one addresses the excitation of the system. In this section we analyze a particular form of excitation, which can be viewed as dragging an impurity through a superfluid. Namely, we consider the following model:
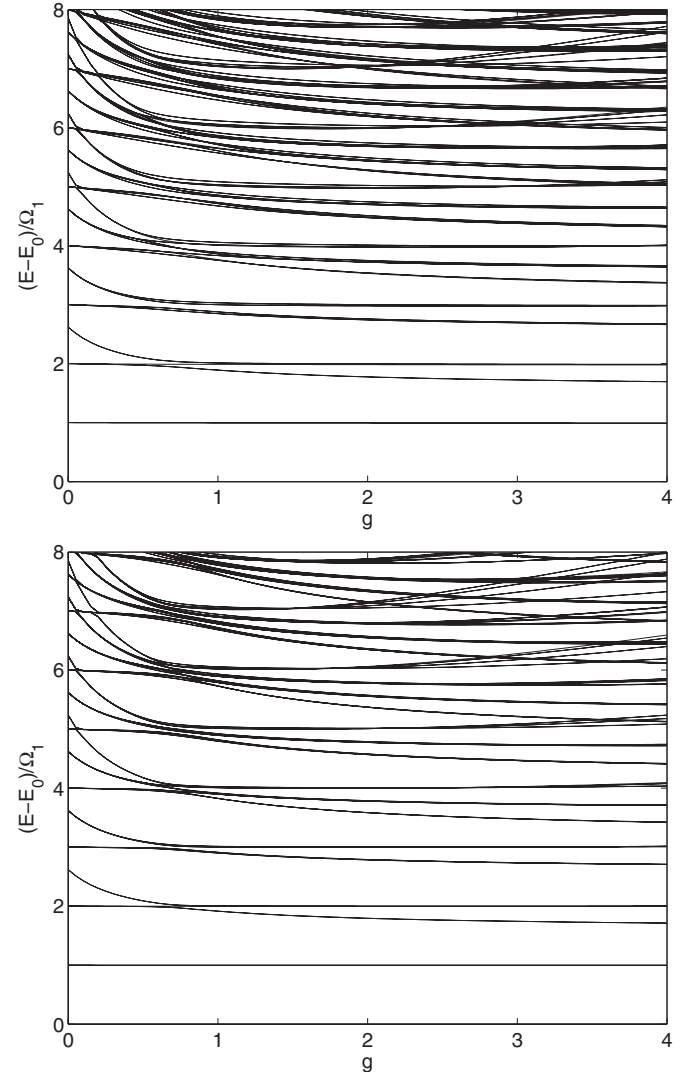
FIG. 8. The low-energy spectrum of the 5-sites BH model for $N=101$ (top) and $N=401$ (bottom). The energy is measured with respect to the ground energy E_0 and scaled with respect to the Bogoliubov frequency Ω_1. The truncation parameter $N'=21$.

$$\hat{H}(t)=\hat{H}_0+\sum_l \hat{n}_l f(l-\omega t),\qquad(33)$$

where $\hat{H}_0$ is the Hamiltonian of the L-sites BH model. (As a physical realization of this model one can think about Bose atoms in a ring optical lattice with a superimposed rotating speckle pattern.) Assuming the system to be initially in the ground (superfluid) state, periodic driving may excite the system and we are interested in details of this process [15–17].

We begin with the case of vanishing interactions and shall assume for simplicity harmonic driving,

$$f(l-\omega t)=\epsilon\cos(2\pi l/L-\omega t).\qquad(34)$$

Changing from the Wannier to Bloch basis, we have,

$$\hat{H}(t) = \hat{H}_0 + \frac{\epsilon}{2}\left(\sum_k \hat{b}_{k+1}^\dagger \hat{b}_k e^{i\omega t} + \text{H.c.}\right), \qquad (35)$$

where $\hat{H}_0$ is given in Eq. (2). For $U=0$ the ground state of (2) is a product state, where all atoms have zero quasimomentum. To be concrete, let us consider again the case $L=3$. Then the excitation process corresponds to the following sequence of transitions:

$$|0,N,0\rangle \to |0,N-1,1\rangle \to |0,N-2,2\rangle \to \cdots ,$$

i.e., atoms are brought one by one to the state with the quasimomentum $k=+1$. Introducing $|\Psi(t)\rangle = \Sigma_{m=0}^N c_m(t)|0,N-m,m\rangle$, this process is described by the system of linear equation on the coefficients c_m,

$$i\dot{c}_m = \delta m c_m + \frac{\epsilon}{2}\left(v_{m+1}e^{i\omega t}c_{m+1} + v_m e^{-i\omega t}c_{m-1}\right), \qquad (36)$$

where

$$\begin{aligned} v_m &= \langle 0,N-m-1,m+1|\hat{b}_{+1}^\dagger \hat{b}_0|0,N-m,m\rangle \\ &= \sqrt{(N-m)(m+1)}. \end{aligned}$$

Equation (36) formally coincides with the Schrödinger equation for a spin in alternating magnetic field and can be solved analytically. In particular, considering the mean energy $E(t) = \langle \Psi(t)|\hat{H}_0|\Psi(t)\rangle$, one has

$$E(t) = E(0) + A[1 - \cos(\tilde{\omega}t)], \qquad (37)$$

where

$$A = \frac{N\delta}{2}\frac{\epsilon^2}{(\delta-\omega)^2 + \epsilon^2}, \quad \tilde{\omega} = \sqrt{(\delta-\omega)^2 + \epsilon^2}. \qquad (38)$$

For the purpose of future comparison, Fig. 9(a) shows time evolution of the mean energy for $g=0$ and $\epsilon=0.2$. A good overall agreement with the analytical solution (37) and (38) is noticed. A deviation from this solution at $\omega \approx 0.75$ is a second-order process, which corresponds to population of the $k=-1$ quasimomentum state through virtual population of the $k=+1$ state. This process has maximal intensity at $\omega = \delta/2$, where the characteristic frequency of oscillations scales as ϵ^2.

We proceed with the case $U \neq 0$. For $U \neq 0$ the ground state of the system is the Bogoliubov state $|\Psi_{m,j}\rangle$ with the quantum numbers $m=j=0$. The upper panel in Fig. 10 shows the transition matrix elements from the ground to all other eigenstates of the system,

$$v(E) = \langle \Psi_E|\hat{b}_{+1}^\dagger \hat{b}_0|\Psi_{0,0}\rangle,$$

which are labelled in the figure by the eigenenergy E. It is seen that the function $v(E)$ is dominated by a single transition to the Bogoliubov state $|\Psi_{1,1/2}\rangle$. Analogously, the strength function for the latter state is dominated by the transition to the Bogoliubov state $|\Psi_{2,1}\rangle$ (middle panel). Thus the dominant excitation process corresponds to the following sequence of transitions:
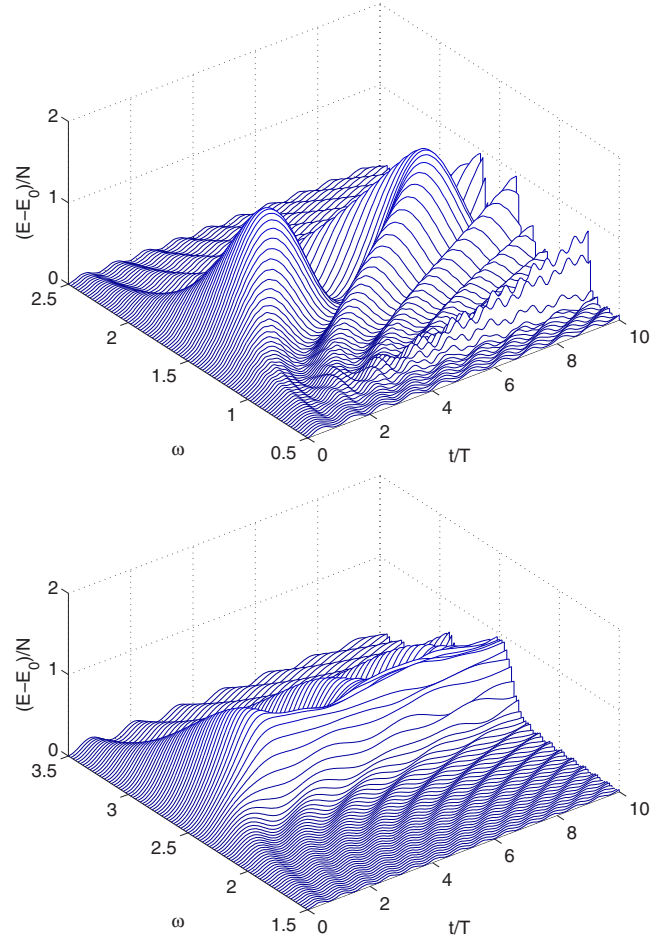
FIG. 9. (Color online) Mean energy of the 3-sites BH model for different values of the driving frequency ω. Parameters are $N=40$, $\epsilon=0.2$, $g=0$ (upper panel) and $g=2$ (lower panel).
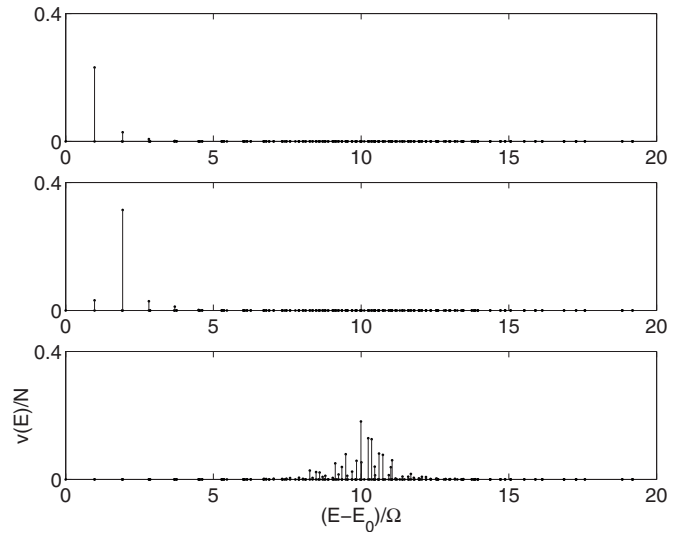
FIG. 10. Transition matrix elements from the Bogoliubov states $|\Psi_{0,0}\rangle$ (top), $|\Psi_{1,1/2}\rangle$ (middle), and $|\Psi_{12,6}\rangle$ (bottom) to all other eigenstates. Parameters are $N=20$ and $g=2$.
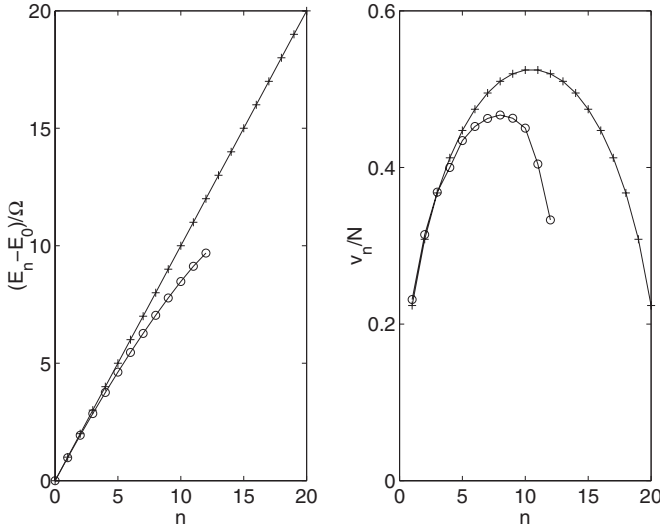
FIG. 11. Energies of the Bogoliubov states $|\Psi_{m,j}\rangle$ with $j=m/2$ (left-hand side) and the transition matrix elements between these states (right-hand side) for $g=0$ (crosses) and $g=2$ (circles), $N=20$.

FIG. 12. (Color online) Phase portrait of the effective system (40) for $g=2$, $\epsilon=0.2$ and driving frequency $\omega=2.2$ (left-hand panel) and $\omega=\Omega\approx2.87$ (right-hand panel). The bottom of the shadowed region [where the model (40) is not applicable] indicates the border of chaos.

$$|\Psi_{0,0}\rangle \rightarrow |\Psi_{1,1/2}\rangle \rightarrow |\Psi_{2,1}\rangle \rightarrow |\Psi_{3,3/2}\rangle \rightarrow \cdots .$$

The indicated sequence reflects an approximate selection rule for the transition matrix elements between Bogoliubov states, which holds if primary quantum number m is smaller than the critical number (29). Introducing $|\Psi(t)\rangle = \Sigma_m c_m(t)|\Psi_{m,m/2}\rangle$, we come back to Eq. (36), where one must substitute δm by the energy of the mth Bogoliubov states with the second quantum number $j=m/2$ and the transition matrix element $v_m=\sqrt{(N-m)(m+1)}$ by the transition matrix element $v_m=\langle\Psi_{m+1,(m+1)/2}|\hat{b}_{+1}^\dagger\hat{b}_0|\Psi_{m,m/2}\rangle$. We compare the energies E_m and the elements v_m for $N=20$ and different values of g in Fig. 11. Note that for $g\neq0$ the number m is restricted to $m<m_{cr}$. Above this critical value Bogoliubov states are destroyed, which also means the absence of any selection rule (see lower panel in Fig. 10).

We shall solve Eq. (36) by employing a semiclassical approach. The semiclassical Hamiltonian of the system (36) obviously reads

$$H_\omega = H_0(I) + \epsilon v(I)\cos(\theta - \omega t), \quad I<I_{cr}, \quad (39)$$

where $H_0(I)$ and $v(I)$ are obtained by interpolating data in Fig. 11. Thus we are faced with the problem of a driven nonlinear oscillator. As known, harmonic driving can excite a nonlinear oscillator only up to a finite $I\leq I^*$. One obtains this maximal value by following the phase-space trajectory of an effective system:

$$H'_\omega = H_0(I) - \omega I + \epsilon v(I)\cos(\theta'), \quad \theta' = \theta - \omega t, \quad (40)$$

originating at $I=0$. Figure 12 shows the phase portrait of the effective system (40) for $g=2$, $\epsilon=0.2$, and two different values of the driving frequency ω. In the right-hand panel, corresponding to $\omega=2.87$ (value of the Bogoliubov frequency Ω at $g=2$), $I^*\approx0.3$ is below the border of chaos $I_{cr}\approx0.5$. Referring to the original quantum system this means that the

excitation process is reversible and involves only a few lowest levels of the Bogoliubov spectrum. If ω is decreased, the nonlinear resonance with the center at $\theta'=0$ moves up and at $\omega\approx2.6$ the upper part of the separatrix trajectory crosses the border of chaos. Thus the system can be efficiently excited from its ground state into the chaotic region, where energy dissipates. With further decrease of the driving frequency, the lower part of the separatrix trajectory detaches the $I=0$ axis and, hence, again only a few lowest levels can be excited. The results of direct numerical simulations of the 3-sites BH model, presented in the lower panel of Fig. 9, fully support the above analytical prediction. It is seen in the figure that excitations are irreversible only in a narrow frequency window $2.4<\omega<2.6$. Outside this window, the system cannot come through the regular part of the spectrum and the excitation process resembles that for $g=0$. We also mention that the frequency interval, where the system resonantly responds to harmonic driving, is shifted towards larger frequencies as compared to the case $g=0$. This shift reflects the square root dependence of the Bogoliubov frequency on the microscopic interaction constant, $\Omega=(2g\delta+\delta^2)^{1/2}$, and may be considered as a test for the Bogoliubov spectrum.

We also studied excitations of the 5-sites BH model (see Fig. 13). For $g=0$ time evolution of the mean energy is similar to that for $L=3$, with two minor differences: (i) the system resonantly responds to a smaller frequency $\omega=\delta_1=1-\cos(2\pi/5)$; (ii) the second-order excitation process corresponds to the population of $k=+2$ quasimomentum state (through virtual population of $k=+1$ state) and is defined by the condition $2\omega=\delta_2=1-\cos(4\pi/5)$. The lower panel in Fig. 13 shows evolution of the mean energy for $g=2.1$. Similar to the case $L=3$, excitations were found to be irreversible in some frequency interval $\omega_{\min}(\epsilon)<\omega<\omega_{\max}(\epsilon)$, shifted to higher frequencies. (Since for $L=5$ the minimal single-
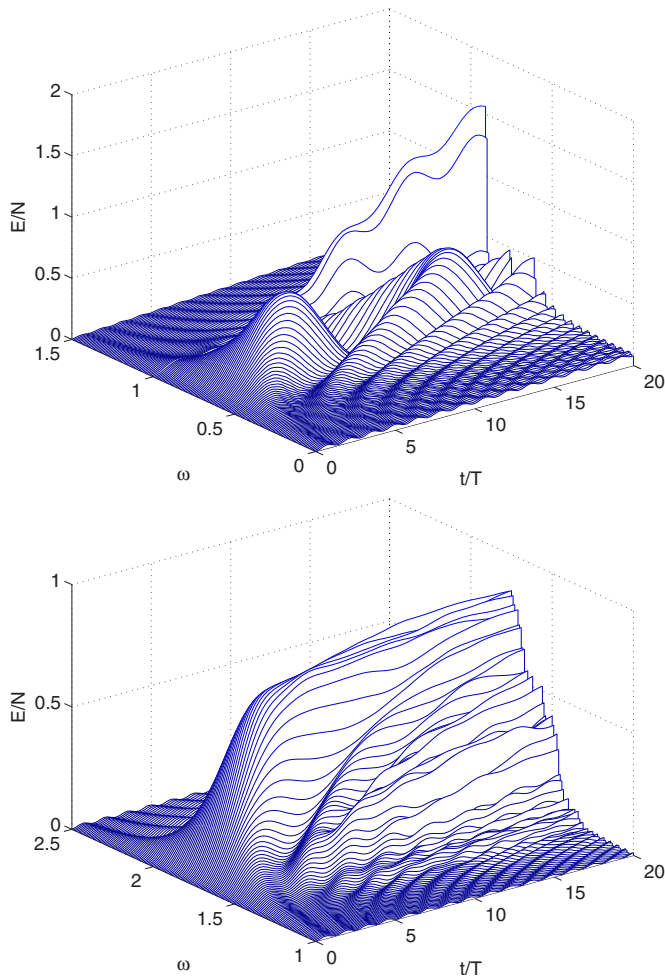
FIG. 13. (Color online) Mean energy of the 5-sites BH model for different values of the driving frequency ω. Parameters are N $=21$, $\epsilon=0.1$, $g=0$ (upper panel) and $g=2.1$ (lower panel).

particle excitation energy δ is smaller than for $L=3$, this frequency shift is even more pronounced in Fig. 13 than in Fig. 9.)

VIII. CONCLUSION

In conclusion, we have analyzed the low-energy spectrum of the BH model with finite number of sites L and finite number of particles N. For infinite number of particles this spectrum is given by the Bogoliubov spectrum, which is usually introduced by using the Bogoliubov–de Gennes transformation. This standard method, however, is rather formal and hides the underlying classical dynamics of the BH model. In this work we use a semiclassical method which, by definition, explicitly refers to the classical dynamics and provides in this way a deeper insight in the structure of the low-energy

spectrum. In particular, it allows one to account for finite size effects, which are of fundamental importance for experiments with cold atoms in optical lattices.

In the present work we are mainly concerned with the 3-sites BH model. An advantage of the 3-sites model is that its classical dynamics can be understood in every detail. In particular, the phase space of the system essentially consists of two regular and one chaotic component in between, where the low-energy regular component is shown to be associated with the Bogoliubov spectrum. We identify the full set of integrals of the motion for this low-energy regular component and, quantizing them, obtain low-energy levels of the quantum BH model. These levels are labelled by two quantum numbers, m and j. The first quantum number m corresponds to the usual Bogoliubov ladder, where the distance between neighboring levels is approximately given by the Bogoliubov frequency Ω (i.e., $E_{m+1,j}-E_{m,j}\sim\Omega$). The second quantum number j labels $(m+1)$ sublevels of the mth Bogoliubov level, where the splitting between sublevels is proportional to the interaction constant g and inverse proportional to the system size N (i.e., $E_{m,j+1}-E_{m,j}\sim g/N$). If we go up the energy axis, the total splitting of the Bogoliubov levels compares the distances between them and the energy spectrum shows a transition from a regular to irregular (chaotic) one.

The described scenario of evolution of the Bogoliubov spectrum into a regular, Bogoliubov-type spectrum and further into a chaotic spectrum also holds for the finite-N BH-model with $L>3$ sites. However, for $L>3$ the border of chaos is essentially lowered due to interactions between different Bogoliubov spectra, associated with different single-particle excitation energies. We analyzed interactions between the spectra by considering the 5-sites BH system, where the critical energy of the transition to chaos is found approximately 10 times smaller than for $L=3$. It is an open problem of how this critical energy scales with the number of sites L. We reserve this problem for future studies, only noting here its formal analogy with the famous Fermi-Pasta-Ulam problem [18].

The identified global structure of the energy spectrum (i.e., the regular Bogoliubov-type spectrum followed by a chaotic spectrum) defines the excitation dynamics of the finite-N BH system. In this work we consider excitations by an external harmonic field. It is shown that the system resonantly responds to the external field when the driving frequency compares the Bogoliubov frequency. If this resonance condition is satisfied, the system rapidly climbs up the Bogoliubov ladder of levels (with the energy increase $\sim t^2$) until it reaches the chaotic region. Starting from this moment the further increase of the energy has a diffusive character. These numerically observed dynamics of the mean energy suggest a simple method for detecting the border of chaos in a laboratory experiment with cold atoms in optical lattices.

[1] L. D. Landau, J. Phys. (USSR) **5**, 71 (1941); N. N. Bogoliubov, *ibid.* **9**, 23 (1947).

[2] A. J. Leggett, Rev. Mod. Phys. **73**, 307 (2001).

[3] L. Cruzeiro-Hansson, H. Feddersen, R. Flesch, P. L. Christiansen, M. Salerno, and A. C. Scott, Phys. Rev. B **42**, 522 (1990).

[4] A. R. Kolovsky and A. Buchleitner, Europhys. Lett. **68**, 632 (2004).

[5] M. Hiller, T. Kottos, and T. Geisel, Phys. Rev. A **73**, 061604(R) (2006).

[6] A. R. Kolovsky, New J. Phys. **8**, 197 (2006).

[7] J. C. Eilbeck, P. S. Lomdahl, and A. C. Scott, Physica D **16**, 318 (1985).

[8] D. Hennig, H. Gabriel, M. F. Jørgensen, P. L. Christiansen, and C. B. Clausen, Phys. Rev. E **51**, 2870 (1995).

[9] K. Nemoto, C. A. Holmes, G. J. Milburn, and W. J. Munro, Phys. Rev. A **63**, 013604 (2000).

[10] R. Franzosi and V. Penna, Phys. Rev. A **65**, 013601 (2001); Phys. Rev. E **67**, 046227 (2003).

[11] P. Buonsante, R. Franzosi, and V. Penna, Phys. Rev. Lett. **90**, 050404 (2003).

[12] This should be opposed to the 2-sites BH model, which is integrable. The different dynamical regimes of the 2-sites BH model (which became a paradigm for multiparticle tunneling phenomena) are discussed, for example, in the review [2].

[13] G. E. Astrakharchik and L. P. Pitaevskii, Phys. Rev. A **70**, 013608 (2004).

[14] This result can also be obtained by using the pure quantum arguments, i.e., by calculating the matrix elements between the relevant Bogoliubov states.

[15] The problem of excitations of cold atoms in a lattice by a periodic driving was addressed earlier in the experimental work [16], followed by theoretical papers [17]. However, while the cited experiment refers to the case of strong atom-atom interactions and small filling factor, here we are interested in the opposite limit of weak interactions and large filling.

[16] T. Stöferle, H. Moritz, C. Schori, M. Köhl, and T. Esslinger, Phys. Rev. Lett. **92**, 130403 (2004).

[17] A. Reischl, K. P. Schmidt, and G. S. Uhrig, Phys. Rev. A **72**, 063609 (2005); A. Iucci, M. A. Cazalilla, A. F. Ho, and T. Giamarchi, *ibid.* **73**, 041608(R) (2006); G. Pupillo, A. M. Rey, and G. G. Batrouni, *ibid.* **74**, 013601 (2006); C. Kollath, A. Iucci, T. Giamarchi, W. Hofstetter, and U. Schollwöck, *ibid.* **97**, 050402 (2006).

[18] See Chaos **15** (1) (2005), special issue devoted to the 50th anniversary of the Fermi-Pasta-Ulam problem.